

OPTICAL STOCHASTIC COOLING IN A LOW ENERGY ELECTRON STORAGE RING FOR A COMPACT X-RAY SOURCE*

Xiaozhe Shen, Peicheng Yu[†], Wenhui Huang, Chuanxiang Tang
Accelerator Laboratory, Department of Engineering Physics,
Tsinghua University, Beijing 100084, China

Abstract

We present the feasibility study of utilizing the Optical Stochastic Cooling (OSC) in a low energy electron storage ring for a compact x-ray source. Owing to the strong effect of the Intrabeam scattering (IBS) and Compton scattering (CS), the equilibrium parameters of the electron beam deteriorate rapidly, which might significantly affect the x-ray photon yield. By utilizing the OSC approach we are able to optimize the beam parameters and enhance the average intensity of the scattered photon yield. Main lattice design, OSC insertion design, and simulations involving IBS, OSC, Synchrotron radiation (SR), and CS are presented in this paper.

INTRODUCTION

Optical Stochastic Cooling (OSC), proposed by Mikhailichenko and Zolotarev [1], provides a competitive method to damp the transverse and longitudinal emittance of the charged beams in a storage ring. The transit-time method of OSC was proposed by Zolotarev and Zholents [2]. Lee and co-workers [3] developed the formalisms and pointed out that the transit-time method would be beneficial to low energy electron beams and proton beam with the energy around 1 TeV. Several laboratories are conducting research actively to demonstrate experimentally the principles of the OSC [4, 5, 6].

In this paper, we present a feasibility study to apply the OSC to a low energy compact laser electron storage ring (LESR), which is utilized as part of a Compton x-ray source [7]. The circumference of the ring is about 15 m, and the electron energy is 50 MeV. The main parameters of the ring are listed in Tab. 1. Owing to the strong effects of Intrabeam scattering (IBS) and Compton scattering (CS) in this storage ring, the beam emittance would grow rapidly in all three directions in the steady mode of the LESR, in which the electron beam is stored for a long period of time. In the horizontal direction, the equilibrium would reach 1.5×10^{-6} m owing to the strong IBS effect; while in the longitudinal direction, the energy spread would arrive at about 1%, mainly due to the effect of CS. Hence, there is a desire to counter-balance these excitation factors in the storage ring and minimize the beam emittance by a fast cooling method, in order to optimize the scattered x-

ray photon yield.

Table 1: Beam parameters for the LESR.

Parameters	Values
Electron energy (E_s), MeV	50
Circumference, m	15
Initial beam	
Horizontal emittance (ϵ_x), nm	20
Energy spread (σ_p)	0.16%
Bunch length (l_b), mm	5.5
Equilibrium (CS / without CS)	
Horizontal emittance (ϵ_x), μm	1.3/7.8
Energy spread (σ_p)	0.8% / 0.32%

MAIN LATTICE

The ring layout is presented in Fig. 1. We place the OSC insertion device in the upper long straight section of the ring, while placing the RF cavity, Interaction Point, and the injection system at the lower one. We keep the lower straight section dispersion-free to ensure beam stability, and adjust the dispersion of the upper straight section to $D_x = 0.13$ m to obtain the maximal cooling rate [8].

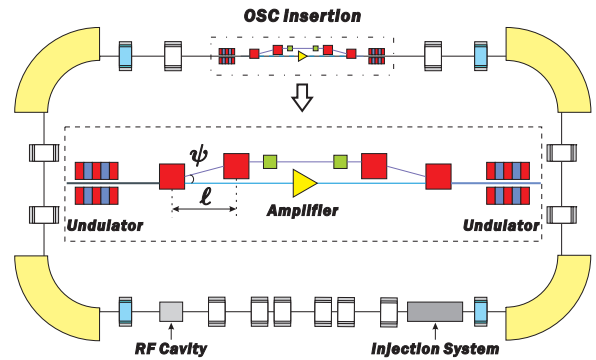


Figure 1: General layout of the storage ring with the OSC insertion.

OSC INSERTION DESIGN

We follow the standard Chicane design with four dipoles and two quadrupoles placed symmetrically at the upper long straight section. In order to obtain an efficient cooling effect, we choose the optimized values of the elements

* Work supported by the Chinese National Foundation of Natural Sciences under Contract no. 10735050, and 10805031.

[†] tpc02@mails.thu.edu.cn

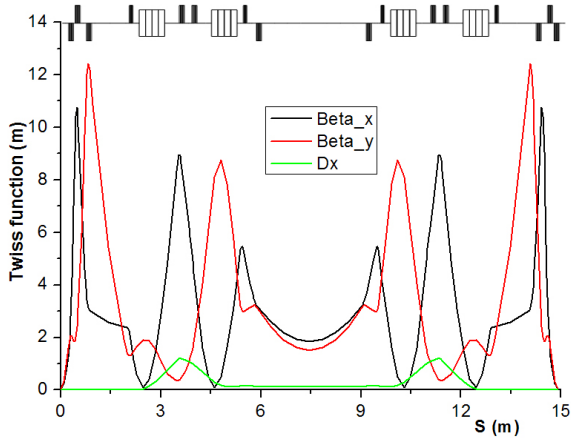


Figure 2: Twiss functions of the ring lattice.

R_{51} , R_{52} , and R_{56} of the Chicane transport matrix to meet the optimized condition for the mean square phase difference averaged over the beam phase space $\Delta\phi^2$ [3, 9]. In the meanwhile, a relatively large bending angle of the Chicane is chosen to obtain a path length increase of the Chicane of $\Delta L \approx \ell\psi^2 = 1.25$ mm. Table 2 presents the parameters for the OSC insertion.

Table 2: Designed parameters for the OSC insertion.

Parameters	Values
Undulator	
Number of periods (N_u)	5
Undulator periods (λ_u), m	0.1
Central magnetic field (B_0), T	0.25
Magnetic deflection parameter (K)	2.33
Amplified photon wavelength (λ), μm	20
Chicane	
Total length (L), m	2.0
Dipole bending angle (ψ), mrad	49
Distance between first 2 dipoles (ℓ), m	0.5
Twiss parameters (at 2nd undulator)	
β_x , m	2.9
D_x , m	0.13
D'_x	0

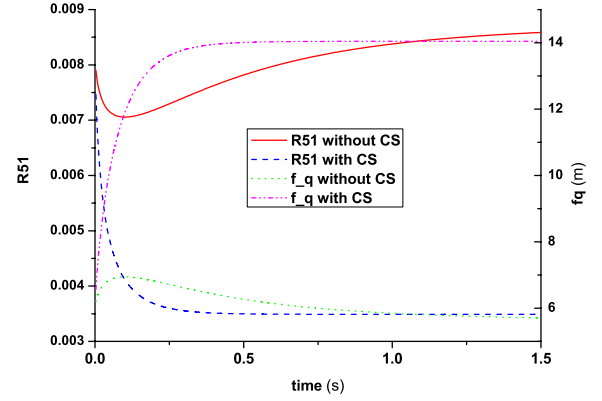
We rely on the two undulators to exchange the energy between the electrons and amplified photons to damp the energy spread; in the meanwhile, transverse cooling is realized by means of the dispersion function D_x and D'_x [8]. Owing to the symmetrical design of the main lattice, D'_x remains zero all through the OSC insertion in our case. However, the maximal values of the symmetrical cooling rates for both directions are still accessible.

Since the maximal cooling rate depends on the transverse emittance ϵ_x and energy spread σ_p , the changes of these quantities during the cooling process would make the cooling rate deviates gradually from its optimized value. To obtain a maximal cooling rate throughout the cooling

process, we have to adjust the gain factor and the bypass parameters during the cooling process [9]. To the first order, the elements of the Chicane transport matrix can be expressed as

$$R_{51} \approx \frac{2\ell\psi}{f_q}, R_{52} \approx \frac{L\ell\psi}{f_q}, R_{56} \approx -2\ell\psi^2 \left(1 + \frac{\ell}{2f_q}\right)$$

where the physical meanings of ℓ , L , and ψ are presented in Tab. 2, and f_q is the focal length of the Chicane quadrupoles. By adjusting the value of f_q we could adjust the corresponding elements to maintain the maximal cooling rate. As shown in Fig. 3, f_q increases about 100% in the time interval of 0.5 s with the CS included. Note that f_q is quite small for the compact storage ring, and its influence on the main lattice should be taken into account in the lattice design.


 Figure 3: Values of R_{51} and f_q as a function of time.

COOLING PROCESS SIMULATION

In order to illustrate the effect of the OSC in the storage ring, we accomplished a simulation including the Synchrotron radiation (SR), IBS, CS, and OSC. The beam phase space evolution is obtained by iterating the instantaneous growth (damping) rates of the four dynamics mechanisms until the equilibrium parameters are achieved. The OSC damping effect is calculated with the optimal cooling condition $\Delta\phi^2 = 1$ throughout the process. The simulation results are presented in Fig. 4 and 5.

For the cases involving the OSC, the OSC mechanism is added right after the beam injection. Figure 4 shows that when the CS and OSC is excluded, the SR is not able to suppress the heating effect of the IBS, until an equilibrium emittance of 1.5×10^{-6} m is achieved, which is about 100 times the initial value. When the OSC is included, the growth of ϵ_x is significantly suppressed, and ϵ_x reaches an equilibrium of 6×10^{-7} m at about 3 s after the injection. Therefore, a growth reduction of 50% is achieved via the OSC. Likewise, the energy spread of 0.23% with a growth

reduction of 30% is achieved. We can see that since the difference in equilibrium between the cases with and without the OSC is significant, our scheme can be utilized to accomplish the proof of principles experiment of the OSC.

Since our preliminary goal is to enhance the x-ray photon yield in the steady mode of the LESR, we likewise accomplish the simulation with the CS included, as is shown in Fig. 5. When the OSC is absent, we can see that ϵ_x evolves from the initial value to an equilibrium at about 1.5×10^{-6} m in 2 s. Moreover, the energy spread reaches as much as 0.8%. When the OSC is included, a lower energy spread of 0.55% is achieved. In the horizontal direction, we likewise achieve a lower equilibrium at about 7×10^{-7} m in less than 1 s. Hence, when the CS is involved, we likewise achieve a 50% growth reduction in the horizontal direction and a 30% growth reduction in the longitudinal direction.

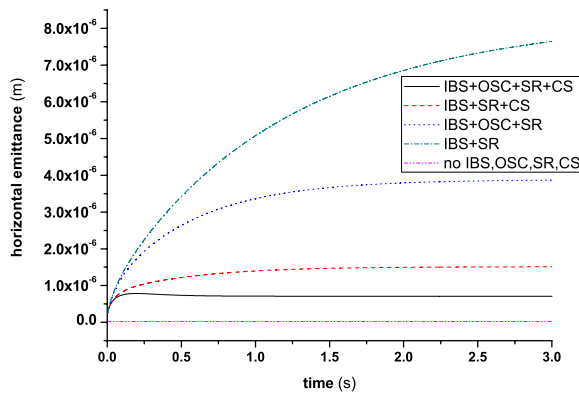


Figure 4: Simulation results for the transverse cooling of the electron beam. IBS is the dominant effect when the OSC is absent. A growth reduction of 50% is obtained with the OSC mechanism.

DISCUSSIONS AND CONCLUSIONS

We present the lattice design and OSC insertion design for the TTX storage ring, in order that an optimized x-ray photon yield can be achieved. With the OSC included in our beam dynamics, we are able to achieve a 50% growth reduction in the horizontal equilibrium and a 30% growth reduction in the longitudinal equilibrium.

In order to maintain the maximal cooling rate condition $\overline{\Delta\phi^2} = 1$, we have to adjust the focal length f_q of the Chicanes quadrupoles. This might affect the whole lattice when f_q is sufficiently small. A detailed scheme should be developed to maintain the local values of the twiss functions, while involving the changes of as few lattice elements as possible.

The path length increase of the Chicane is set to $\Delta L \approx 1.25$ mm, which requires that the corresponding total signal delay of the optical parametric amplifier be less than 4 ps. This challenging constraint should be met in our fu-

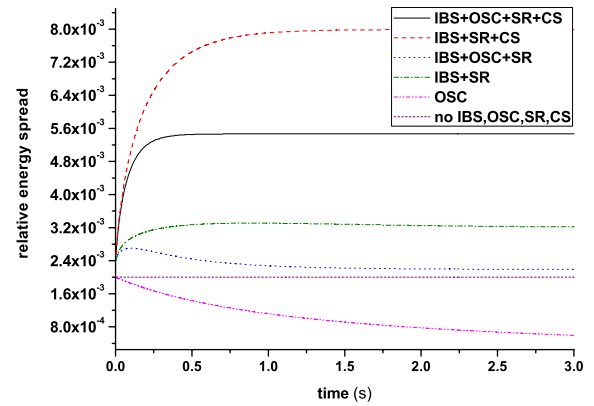


Figure 5: Simulation results for the longitudinal cooling of the electron beam. CS is the dominant effect when the OSC is absent. A growth reduction of 30% is obtained with the OSC mechanism.

ture study of the optical amplifier.

Furthermore, we do not consider the effect of the undulator on the ring lattice in this paper. Owing to the relatively large strength of the undulator, twiss function might change significantly near the OSC insertion. Moreover, the undulator can affect the momentum compaction of the storage ring [10], which might change the beam length equilibrium, thereby affects the cooling rate. We plan to further explore these effects in our future study.

The authors are greatly indebted to Dr. Yunkai Zhang, Dr. Fuhua Wang, and Dr. C. Tschalaer for helpful instructions and fruitful discussions.

REFERENCES

- [1] A. Mikhailichenko and M. Zolotarev, *Phys. Rev. Lett.* **71**, 4146–4149 (1993)
- [2] M. Zolotarev and A. Zholents, *Phys. Rev. E* **50**, 3087–3091 (1994)
- [3] S. Y. Lee, Y. Zhang, and K. Y. Ng, *NIM - A* **532**, 340–334 (2004)
- [4] W. A. Franklin, et al. in *Proceedings of COOL 2007*, Bad Kreuznach, Germany, 117–120 (2007).
- [5] E. G. Bessonov, M. V. Gorbunkov, and A. A. Mikhailichenko, in *Proceedings of EPAC-06*, Edinburgh, Scotland, 1483–1485 (2006)
- [6] M. Babzien, I. Ben-Zvi, I. Pavlishin, I. Pogorelsky, V. Yaki-menko, A. Zholents, M. Zolotarev, *NIM - A* **532**, 345–347 (2004)
- [7] P. Yu, Y. Wang and W. Huang, in *Proceedings of EPAC-08*, Genoa, Italy, 187–189 (2008)
- [8] F. Wang and C. Tschalaer, MIT Internal Report, B/IR#08-02 (2008)
- [9] C. Tschalaer, MIT Internal Report, B/IR#07-02 (2008)
- [10] S. Y. Lee, et al. *Rev. Sci. Instrum.* **78**, 075107 (2005)